Ab Initio Potential Energy Surface and Vibrational Energies of H_3O^+ and Its Isotopomers†

Xinchuan Huang,‡ Stuart Carter,§ and Joel M. Bowman*,‡

Cherry L. Emerson Center for Scientific Computation and Department of Chemistry, Emory University, Atlanta, Georgia 30322 and Department of Chemistry, University of Reading, Reading, RG62AD, U.K.

Received: March 5, 2002; In Final Form: May 7, 2002

We report a new full dimensional potential energy surface for the hydronium ion (H_3O^+). This surface is constructed by a least-squares fit of ab initio electronic energies obtained using the CCSD(T) method with an aug-cc-pVTZ basis set, augmented by some calculations using an aug-cc-pVQZ basis set. The calculated inversion barrier is 693 cm^{-1}. Full dimensional vibrational calculations are reported using the new surface for H_3O^+, D_3O^+, H_2DO^+, and HD_2O^+ using the codes RVIB4 and MULTIMODE. Comparison with all available experimental data on both splittings and vibrational energies shows significant improvement over our previous calculations using the OSS3(p) potential. A number of vibrational band energies and splittings not measured experimentally are reported for D_3O^+, HD_2O^+, and H_2DO^+.

I. Introduction

Interest in the hydronium ion H_3O^+ ranges from its role in aqueous solution chemistry[1] to its proton transferring function in biological systems[2] to its possible presence in dense interstellar clouds.[3,4] In the electronic ground state X (1^1A_1), the global minimum of H_3O^+ is of C_{3v} symmetry.[5] This pyramidal geometry implies a double minimum, as in the case of NH_3, and thus the possibility of the tunneling motion of the O atom via the inversion (umbrella) mode through a barrier separating these equivalent minima. As is well-known, this tunneling results in doublet splittings. These splittings, also known as inversion doublets, have been observed in the IR spectrum of H_3O^+ for all of the fundamental vibrational states, as well as the zero-point level. Two vibrations, the O−H symmetric stretching mode (ν_1) and inversion mode (ν_2), belong to A_1 symmetry, while the O−H antisymmetric stretching modes (ν_3 band) and deformation modes (ν_4 band) are of E symmetry.

In 1977 Schwarz reported the approximate ν_3 band origin in a low-resolution spectrum.[6] Six years later, Begemann identified the accurate origins of this mode.[7] In this high-resolution IR spectrum of H_3O^+ the ν_3 band origins were reported at 3530.16 ($0^+ \leftarrow \nu_3^+$) and 3513.84 cm^{-1} ($0^- \leftarrow \nu_3^-$), respectively, where the superscript + (−) indicates the lower (upper) level of the doublet. In 1987, origins of the ν_4 band were first reported at 1625.95 ($0^+ \leftarrow \nu_4^+$) and 1638.53 cm^{-1} ($0^- \leftarrow \nu_4^-$) by Gruebele et al.[8] employing diode laser velocity modulation spectroscopy. The ν_1 band origins were determined two years ago by Tang and Oka.[9] Using a difference frequency laser spectrometer, they reported the ν_1 origins at 3389.66 ($0^- \leftarrow \nu_1^+$) and 3491.17 cm^{-1} ($0^+ \leftarrow \nu_1^-$).

The splittings of the inversion-tunneling mode ν_2 have received considerable attention experimentally.[10−15] The absorption spectrum of the $0^\pm$, $1^\pm$, and $2^\pm$ energy levels of this band have been measured by several groups. The first observation of the $1^- \leftarrow 0^+$ transition was reported at 954.4 cm^{-1} by Haese and Oka.[10] Additionally, Liu and Oka[11] located the $1^- \leftarrow 1^+$ band origin at 373.23 cm^{-1}. These data together with other reports from Davies et al.[12,13] and Liu et al.[14] led to a determination of the ground-state inversion splitting of 55.35 cm^{-1}. This analysis also led to a prediction of the ground-state inversion spectra in the far-infrared region, and the inversion-rotation spectra in the millimeter-wave region, both of which are needed to aid in the detection of H_3O^+ in interstellar space. Based on the predictions, the pure inversion spectra of H_3O^+ was directly observed[15] in the far-infrared region at around 55 cm^{-1}. The ν_2 and ν_3 fundamental bands (and splittings) have been recorded for D_3O^+.[16,17] For two partially deuterated hydronium ions H_2DO^+ and HD_2O^+, no experimental frequencies have yet been reported.

In parallel with the experimental work on H_3O^+ there have also been numerous theoretical studies of this ion. Before 1980, theoretical research focused on the C_{3v} minimum and D_{3h} inversion saddle point (ISP) geometries, harmonic frequencies, and inversion barrier height. The inversion barrier was estimated in the range from 385 to 1679 cm^{-1}, based on CNDO/2 and CISD, CEPA PNO, etc. ab initio methods.[18−29] Bunker, Spirko, and Kraemer have, in a series of papers,[16,30−33] applied a reduced dimensionality, invertor Hamiltonian to obtain vibrational energies and splittings of H_3O^+, D_3O^+, H_2DO^+, and HD_2O^+. The most recent work[33,34] utilized a combination of ab initio calculations and adjustments to fit experiment to obtain two potentials, with inversion barrier heights of 711 and 743 cm^{-1}.

The first attempt at a full dimensional quantum calculation of five low-lying vibrational states of the deuterated hydronium ion, D_3O^+, was reported by Gomez and Pratt[35] in 1998. Their calculation, which was not intended to be of spectroscopic accuracy, i.e., converged to within less than 10 wavenumbers, used two semiempirical full dimensional potentials, one due to Stillnger et al.[36] and another due to Ojamae et al.[37] The splitting of the ground state was estimated to be 15 cm^{-1} using the fixed-node diffusion Monte Carlo method. This result is in good agreement with an experimental estimate;[16] however, the authors implied that this apparent quantitative agreement was fortuitous, because the error in their calculated splitting is of the order of the splitting itself.

We recently reported[38] full dimensional calculation of vibrational energies of H_3O^+ and D_3O^+ using the OSS3(p)

† Part of the special issue "John C. Tully Festschrift".

* Corresponding author. E-mail: bowman@euch4e.chem.emory.edu.
‡ Emory University.
§ University of Reading.

10.1021/jp020619i CCC: $22.00
Published on Web 06/27/2002

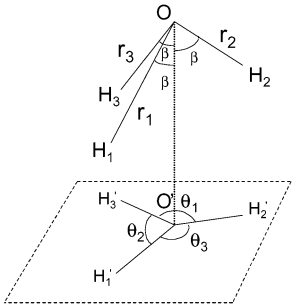

Figure 1. Coordinates used to express the potential of H_3O^+ as described in detail in the text.

potential.[37,39] This potential was originally developed for simulations of water with excess protons. A full dimensional potential for $H_5O_2^+$ was obtained using MP2 ab initio calculations at approximately 2950 configurations, and a fit was made to these ab initio calculations. Among these configurations, there were several hundred corresponding to the free fragments H_3O^+ and H_2O. Thus, by separating these two fragments and freezing H_2O at its (OSS3(p)) equilibrium geometry, we isolated the H_3O^+ potential and used it in our vibrational calculations. We determined the equilibrium and saddle point structures of H_3O^+. The equilibrium geometry is of C_{3v} symmetry with r_{OH}= 0.9794 Å and $\theta_{HOH} = 111.84°$, in good agreement with the geometry reported by Ojamae et al.[37] which agrees well with results obtained directly from the ab initio calculations. The inversion saddle point geometry, of D_{3h} symmetry, has $r_{OH} = 0.9871$ Å, which is longer than the C_{3v} bond length. (Previous calculations[16,18,33] showed a decrease in this bond length compared to the C_{3v} equilibrium value.) Also, the barrier height for inversion is 1352.01 cm^{-1}, which is considerably larger than estimates of ca. 700 cm^{-1} noted above and also from an ab initio calculation[40] (700 cm^{-1}). Thus, from this error in the barrier height alone it is clear that the OSS3(p) potential for H_3O^+ is not of spectroscopic accuracy, and in fact our full dimensional vibrational calculations using this potential were in poor agreement with experiment.[38]

In this paper, we report a new full dimensional potential energy surface (PES) for H_3O^+, based on high-quality ab initio calculations and a precise fit to the electronic energies. The fitted PES is used in full dimensional vibrational calculations of H_3O^+, H_2DO^+, HD_2O^+, and D_3O^+ using RVIB4[41,42] and MULTIMODE.[38,43−46]

This paper is organized as follows. The details of the ab initio calculations, the fitting, and the properties of the fitted potential for H_3O^+ are described in section II. The codes to perform the vibrational calculations, RVIB4 and MULTIMODE, and the basis sets, etc. are briefly described in section III. In section IV we present and discuss the results of the vibrational calculations and the comparisons with available experimental data. A summary and concluding remarks are given in section V.

II. Potential Energy Surface

The strategy we used to construct the potential energy surface for H_3O^+ follows in detail the one used very recently by Leonard et al. for NH_3.[42] The six internal coordinates are the three O−H bond lengths r_1, r_2, and r_3, a trisector angle β, and two angles θ_2 and θ_3 which are the angles between two pairs of OH bonds when projected onto a plane perpendicular to the trisector axis. Figure 1 shows these coordinates, and we note that β ranges from 0 to π, and $\theta_1 + \theta_2 + \theta_3 = 2\pi$. The angles θ_2 and θ_3 were chosen as independent variables, and this choice distinguishes r_1 from r_2 and r_3.

TABLE 1: Geometry Optimization (Å and deg) of H_3O^+ Minimum (MIN) and Inversion Saddle Point (ISP) Using the Indicated Method and Basis

	C_{3v} MIN		D_{3h} ISP	
method/basis	r_{OH}	β	r_{OH}	barrier (cm^{-1})
CCSD(T)/6-31G++	0.9786	106.2	0.9721	606
CCSD(T)/VDZ	0.9841	109.5	0.9761	1187
CCSD(T)/VTZ	0.9779	107.4	0.9701	755
CCSD(T)/aug-cc-pVTZ	0.9792	107.4	0.9712	803
CCSD(T)/aug-cc-pVQZ	0.9765	107.1	0.9692	709
CCSD/aug-cc-pVTZ	0.9769	107.2	0.9694	765
BCCD(T)/aug-cc-pVTZ	0.9791	107.5	0.9712	802
BCCD/aug-cc-pVTZ	0.9768	107.1	0.9692	763
MP2/aug-cc-pVTZ	0.9795	107.4	0.9715	764
MP4/aug-cc-pVTZ	0.9797	107.5	0.9717	809
CI/aug-cc-pVTZ	0.9736	106.8	0.9666	711
QCI(T)/aug-cc-pVTZ	0.9793	107.5	0.9712	804
HF/aug-cc-pVTZ	0.9602	104.7	0.9559	447
CEPA(3)/aug-cc-pVTZ	0.9761	107.1	0.9687	757
ACPF/aug-cc-pVTZ	0.9773	107.3	0.9696	780

Note that qualitatively the three bond length coordinates are related to the modes of O−H stretching modes, the two in-plane bond angles θ_2 and θ_3 correspond to the deformation modes, and β describes the inversion mode. The potential is symmetric with respect to reflection of β about π and also with respect to exchange of the three H atoms. Therefore, for nonplanar geometries, five symmetry equivalent grid points can be determined from a single geometry.

The ab initio calculations were done using MOLPRO 2000[47] and the CCSD(T) method, after conducting a survey of methods and basis sets. The results of this survey, restricted to the geometry of minimum and geometry and relative energy of the inversion saddle point, are given in Table 1. As seen, the barrier height ranges from a low HF value of 447 cm^{-1} to a high value of 1187 cm^{-1} for a small basis CCSD(T) calculation. For higher level calculations the barrier heights are in the range 709−809 cm^{-1}. For extensive calculations we chose the CCSD(T) method with the aug-cc-pVTZ basis[48] to determine a potential energy surface. Some calculations were also done with the aug-cc-pVQZ basis (see below for details) to more accurately characterize the inversion saddle point region. A potential energy surface based on calculations using both basis sets is the one that is used in most of our vibrational calculations.

The ab initio energies were fit by the functional form used by Leonard et al. for NH_3[42]

$$V(r_1,r_2,r_3,\theta_2,\theta_3,\beta) = \sum_{i,j,k,l,m,n} C_{ijklmn} f(r_1)^i f(r_2)^j f(r_3)^k g(\theta_2)^l g(\theta_3)^m h(n,\beta) \quad (1)$$

where

$$g(\theta) = \theta - \frac{2}{3}\pi, h(n,\beta) = \cos\left[n\left(\beta - \frac{1}{2}\pi\right)\right],$$
$$f(r) = 1 - \exp[-0.5(r - 1.84)]$$

The reference geometry used in these functions, $\beta = \pi/2$, $\theta_1 = \theta_2 = \theta_3 = 2\pi/3$, $r_1 = r_2 = r_3 = 1.84$ bohr, are average values of these coordinates at the minimum and saddle point geometries.

The indices i, j, k, l, m, and n are all integers, with the restriction $0 \le i, j, k \le 4$, $0 \le l, m \le 6$, $0 \le n \le 5$, exactly as done previously. Thus, there are 324 coefficients to be determined in eq 1. (The symmetric equivalences among the three H atoms noted reduce the number of independent coefficients to 98; however, this symmetry was not imposed on the fit.)

Ab initio calculations with the aug-cc-pVTZ basis were done at 129 symmetry-unique grid points, including the precisely determined minimum and inversion saddle point. Those points were scattered around the C_{3v} minimum and the D_{3h} saddle point geometries with symmetry-unique values of r_{OH} equal to 1.54, 1.69, 1.84, 1.94, 2.14, and 2.44 bohr. From this set of grid points a full set of 568 grid points was generated by making use of symmetry. The coefficients in eq 1 were obtained using the full set of aug-cc-pVTZ energies, and a second fit was done using a mixed set of 76 aug-cc-pVTZ and 53 aug-cc-pVQZ at and in the vicinity of the inversion saddle point. (These two sets were combined by using the energies relative to the respective minima.)

III. Vibrational Calculations

The codes MULTIMODE and RIVIB4 were used to obtain vibrational energies of H_3O^+ and D_3O^+. RVIB4 is limited to tetraatomic molecules and with potentials given in form of eq 1; however, no further approximations are made in this code and so the results from this code, when converged, are "exact" for a given potential. MULTIMODE is a general code that can be applied to molecules larger than tetraatomics; however, it makes some approximations to the potential (as described below), and so converged results from this code are not "exact". Thus it is important to test the accuracy of MULTIMODE by comparing results using it to those using RVIB4. Brief descriptions of these codes are given next.

MULTIMODE has been described in detail previously,[43−46] including the recent modifications that were necessary to describe motion in a multidimensional double well.[38] In brief, MULTIMODE is based on the full Watson Hamiltonian,[48] which is an exact Hamiltonian for rovibrational motion, given in terms of mass-scaled normal modes Q_i. A key feature of MULTIMODE that makes calculations of fairly large molecules feasible is the representation of the full N-mode potential by an exact hierarchical series of mode-coupling terms:

$$V(Q_1,Q_2,...,Q_N) = \sum_i V^{(1)}{}_i(Q_i) + \sum_{ij} V^{(2)}{}_{ij}(Q_i,Q_j) + \sum_{ijk} V^{(3)}_{ijk}(Q_i,Q_j,Q_k) + \sum_{ijkl} V^{(4)}{}_{ijkl}(Q_i,Q_j,Q_k,Q_l) + ...$$

where the *one-mode representation* of the potential contains only $V^{(1)}{}_i(Q_i)$ terms, i.e., the potential along cuts of the normal coordinates, the *two-mode representation* of the potential contains those terms plus the $V^{(2)}{}_{ij}(Q_i,Q_j)$ terms where any pairs of normal modes vary, etc. In the present calculations, for which there are six modes, the series is truncated at the four-mode representation. This representation of the potential makes the dimensionality of integrals involving V at most 4, for any number of normal coordinates.

Eigenvalues and eigenfunctions of the Watson Hamiltonian were obtained using the "VCI" approach. All of these begin with a vibrational self-consistent field (VSCF) Hamiltonian, for the ground vibrational state configuration interaction method, denoted VCI, uses the orthonormal basis of eigenfunctions of a single VSCF Hamiltonian, usually the one for the ground state. The size of the VCI Hamiltonian matrix grows nonlinearly with the size of the molecule, and the numerical evaluation of the matrix elements can become very time-consuming. Thus, numerical quadratures are done using "potential optimized" quadratures, as described in detail elsewhere.[45]

To use MULTIMODE, a reference stationary point, at which a normal mode analysis is done, must be specified. For hydronium, where tunneling splittings are large, the obvious choice for the stationary point is the inversion saddle point, which is of D_{3h} symmetry. This choice treats the two C_{3v} minima equivalently and can, as a result, give a proper description of the tunneling dynamics. The normal mode corresponding to the imaginary frequency is the mode that spans the two minima and is denoted Q_1. (In the present calculation this mode is the inversion mode.) This is a large-amplitude mode, and so a large basis as well as a large number of quadrature points are needed for this mode. Also, since the normal modes of saddle point differ from those of the minimum, extraordinary coupling is to be expected. To deal with these new aspects of the calculation, several new features were developed. First, the numerical basis for the large-amplitude mode was obtained using a relatively large primitive harmonic oscillator basis with a frequency that is user-supplied. The numerical basis contains functions that span both minima and are symmetric or antisymmetric about $Q_1 = 0$. In the method to couple this mode to the five other normal modes, a change was made in the scheme to determine the excitations in each mode to allow much more excitation in the Q_1 mode than was previously possible in earlier versions of MULTIMODE. Second, the one-dimensional potentials for the five real-frequency modes were optimized in a new way. Instead of simply taking cuts of the potential along each mode with the other mode held fixed at zero, they were optimized with respect to the mode Q_1, as follows. For each value of Q_j, $j = 2-6$, the potential was minimized with respect to Q_1. Thus, for example, the potentials for the high-frequency O−H stretching modes approach their shapes at the true minima, which are actually stiffer than at the saddle point.

For H_3O^+ and its isotopomers, the largest bases used consisted of 21 numerical functions in Q_1, obtained from a primitive basis of 32 harmonic oscillator functions. For modes 2−4, nine numerical basis functions were used per mode, contracted from 18 primitive harmonic oscillator functions. For the last two modes, 5 and 6, 18 primitive harmonic oscillator functions were contracted to 10 numerical basis functions. Optimized quadrature points were determined for all modes using the techniques described in detail elsewhere.[44] The orders of the four C_{2v} symmetry blocks of the Hamiltonian matrix for this basis were 5099 (A_1), 4394 (B_2), 4528 (B_1), and 3814 (B_2). The total CPU time for the calculation of eigenvalues and eigenvectors was 3 h, 43 min on a Compaq Alpha workstation (667 MHz processor speed). Smaller bases were also considered to test convergence of the eigenvalues, and based on those tests the results, to be shown in the next section, appear to be converged to better than 1 cm^{-1}.

Vibrational calculations for H_3O^+ and D_3O^+ were also performed using RVIB4.[41,42] This code uses a variational procedure expressed in internal coordinates specifically designed for tetraatomic molecules described by three bond distances, the angle β, and the two in-plane angles θ_2 and θ_3 defined above. The resulting kinetic energy operator in these coordinates is exact, within the limitations of the Born−Oppenheimer approximation. The potential energy is written as a polynomial in these coordinates, relative to a planar (D_{3h}) reference. Because of this, it is possible to transform both kinetic and potential energy integrals during the course of the calculations.

The $J = 0$ energy levels are computed by carrying out systematic contractions of the basis functions. Each contraction utilizes a model kinetic energy operator, derived by constraining the nonparticipating coordinates to their equilibrium values. To supplement this kinetic energy, a subset of the total potential energy is used which only involves the participating coordinates

TABLE 2: Optimized Geometries (Å and deg) and Energies (cm^{-1}) of H_3O^+ C_{3v} Minimum (MIN) and D_{3h} Inversion Saddle Point (ISP) from Direct ab Initio Calculations Indicated or Potential Energy Surface as Described in the Text

	$C3v$ MIN			D_{3h} ISP	
	r_{OH}	β	∠H−O−H	r_{OH}	barrier (cm^{-1})
aug-cc-pVTZ	0.9792	72.6	111.4	0.9712	803
PES-1	0.9789	72.4	111.3	0.9708	783
aug-cc-pVQZ	0.9765	72.9	111.7	0.9692	709
PES-2	0.9782	72.6	111.5	0.9686	693
OSS3(p)	0.979	73.0	111.8	0.987	1352

of the contraction scheme in question. There is one exception to this: since the stretch-only potential only probes the true minimum for a value of the umbrella angle of 72°, the potential used in the stretching contraction scheme is "effective" over the complete range of β. We have demonstrated that such a series of contraction schemes leads to $J = 0$ energy levels which are converged to better than 0.1 cm^{-1} for energies to 10 000 cm^{-1}.

IV. Results and Discussion

The least-squares fits to the CCSD(T)/aug-cc-pVTZ calculations and the combination of CCSD(T)/aug-cc-pVTZ and aug-cc-pVQZ calculations, described above, are denoted PES-1 and PES-2. For both fits the average and root-mean-square fitting errors were 8 and 11 cm^{-1}, respectively, for all 568 energies, up to 60 000 cm^{-1}, with a maximum fitting error of 50 cm^{-1}. A comparison of the geometries and energies of the minimum and inversion saddle point obtained directly from the ab initio calculations and for PES-1 and PES-2 is given in Table 2. As seen, the major difference between PES-1 and PES-2 is the inversion barrier height, with the one for PES-1 being 90 cm^{-1} higher than that for PES-2. This is just a reflection of the lower barrier height obtained with the aug-cc-pVQZ basis. Note that the fitted potentials reproduce the corresponding, directly optimized ab initio geometries of the minimum and saddle point to within 0.001 Å and 0.2°. The PES-1 and PES-2 barrier heights are respectively 20 and 16 cm^{-1} lower than the corresponding ab initio ones, due to slight fitting errors. The barrier height of the OSS3(p) potential is much larger than any of the ab initio results, confirming previous assessments that the OSS3(p) barrier of 1352 cm^{-1} was too large.[35,38]

The ab initio (aug-cc-pVTZ basis) normal mode frequencies and those for PES-1 and PES-2 at the minimum and inversion saddle point are given in Table 3. (Computer limitations prevented us for doing a normal mode analysis with the aug-cc-pVQZ basis.) As seen, the results for PES-1 agree well with the direct ab initio ones; i.e., differences are between 0 and 15 cm^{-1}. Also, the normal mode frequencies for PES-1 and PES-2 are in very good agreement with the exception of the lowest frequency umbrella mode at the minimum, where the difference is 35 cm^{-1}. This may be a reflection of the lower barrier height for PES-2 compared to PES-1.

The normal mode eigenvectors corresponding to the imaginary frequency and the symmetric stretch at the saddle point are plotted in Figure 2. From symmetry considerations it is clear that the configuration of the global minima can be described by these two inversion saddle point normal modes, denoted Q_1 and Q_4. A contour plot of the potential (PES-2) in these two normal modes is given in Figure 3. It is interesting that the "reaction" path connecting the two minima and the saddle point is highly curved. Clearly, to accurately describe the vibrations of H_3O^+ using the saddle point normal modes requires a large

TABLE 3: Harmonic Frequencies (cm^{-1}) of H_3O^+ Normal Modes at the Inversion Saddle Point and Minimum from the Indicated Source[a]

		deformation		OH sym	OH antisym stretch	
	umbrella mode 1	mode 2	mode 3	stretch mode 4	mode 5	mode 6
			Inversion Saddle Point			
ab initio[b]	726i	1628	1628	3642	3793	3793
PES-1	695i	1628	1628	3651	3808	3808
PES-2	662i	1633	1633	3664	3819	3819
OSS3(p)	1057i	1185	1185	3093	3809	3809
			Minimum			
ab initio[b]	924	1701	1704	3590	3685	3685
PES-1	916	1693	1693	3578	3691	3691
PES-2	881	1693	1693	3582	3695	3695
OSS3(p)	972	1639	1639	3045	3711	3711

[a] The character of each normal mode is indicated. [b] CCSD(T)/aug-cc-pVTZ

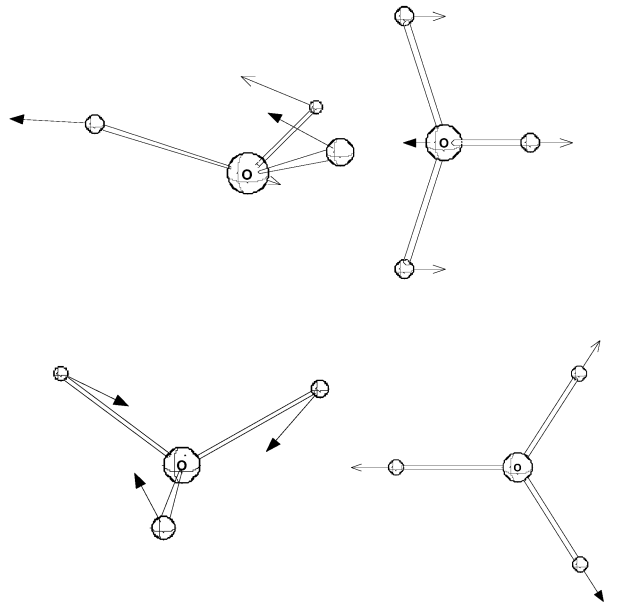

Figure 2. Umbrella normal mode (top) and the OH symmetric stretch normal mode (bottom) at the C_{3v} minimum (left) and at the D_{3h} inversion saddle point (right).

basis in the inversion mode and coupling to other modes. As noted in the previous section, MULTIMODE is run with the normal modes of the inversion saddle point.

We now present results of vibrational calculations for H_3O^+ and D_3O^+ for which there are limited experimental data. We also present results for the mixed isotopomers H_2DO^+ and HD_2O^+ for which no experimental data have been reported.

H_3O^+ and D_3O^+. The experimental and calculated vibrational energies (using PES-2) of the four fundamentals (two of which are doubly degenerate) and the overtone of the umbrella mode are given for H_3O^+ and D_3O^+ in Table 4. The results from MULTIMODE and RVIB4 (which are "exact") are generally in very good agreement with each other. The one exception is the doubly degenerate antisymmetric stretch mode, ν_3. The energies from MULTIMODE are not exactly degenerate, as they should be (for both the "+" and "−" states). For H_3O^+ and D_3O^+ the deviations from degeneracy are 4 and 7 cm^{-1} and 3 cm^{-1}, respectively. This error is evidently due to a slight error in the four-mode representation of the potential for this mode. The error leads to two values of the splitting of the ν_3 fundamental: 32 and 29 cm^{-1} for H_3O^+ and (fortuitously one value) 8 cm^{-1} for D_3O^+. These are, nevertheless, close to the

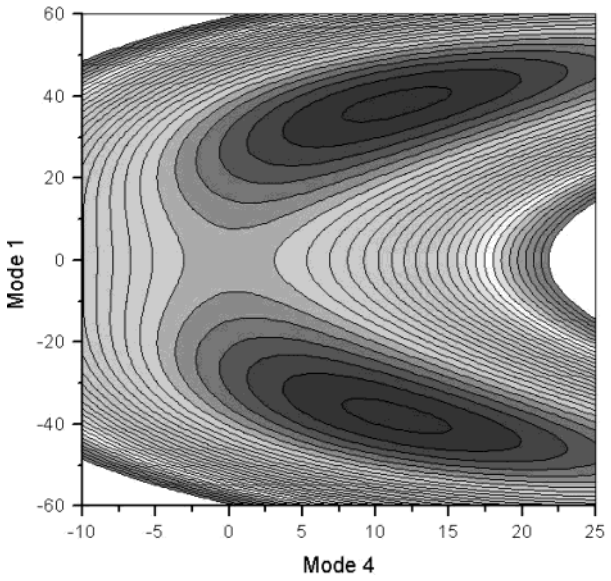

Figure 3. Contour plot of the PES-2 potential as a function of the saddle point umbrella (mode 1) and OH symmetric stretch (mode 4) normal modes.

TABLE 4: Comparison of Experimental and Calculated Vibrational Energies (cm^{-1}) of H_3O^+ and D_3O^+ Obtained from RVIB4 and MULTIMODE (MM) Using PES-2[a]

	MM		RVIB4		EXP			exptl
	(+)	(−)	(+)	(−)	(+)	(−)	split	split
				H_3O^+				
ground state	0	41	0	41	0.0	55.35	41	55.35[b]
ν_2	578	918	580	917	581.17	954.40	337	373.23[c]
$2\nu_2$	1421	1971	1421	1971	1475.84		550	
ν_4	1623	1675	1623	1673				
					1625.95	1693.87	50	67.92[d]
	1623	1675	1623	1673				
ν_1	3387	3420	3386	3418	3445.00	3491.17	33	46.16[e]
ν_3	3527	3559	3522	3550				
					3535.56	3574.29	28	38.73[f]
	3523	3552	3522	3550				
				D_3O^+				
ground state	0	10	0	10	0.0	15.35	10	15.35[g]
ν_2	469	631	469	631	453.74	645.13	162	191.39[h]
$2\nu_2$	974	1329	974	1328			354	
ν_4	1193	1207	1193	1193				
							13	
	1193	1207	1193	1206				
ν_1	2449	2458	2448	2457			9	
ν_3	2621	2629	2618	2624				
					2629.65	2639.59	6	9.94[i]
	2618	2626	2618	2624				

[a] (+) and (−) indicate the parity of each doublet. [b] Reference 14. [c] Reference 11. [d] Reference 8. [e] Reference 9. [f] Reference 7. [g] Reference 16b. [h] Reference 16a. [i] Reference 17.

correct result (from RVIB4) of 28 cm^1 for H_3O^+ and 7 cm^{-1} for D_3O^+. Before discussing the comparison with experiment, note that the RVIB4 zero-point energies for H_3O^+ and D_3O^+ are 7435 and 5462 cm^{-1}, respectively. (The results from MULTIMODE are 7431 and 5457 cm^{-1}, in very good agreement with the RVIB4 energies.)

The agreement with experiment generally ranges from excellent to very good for both the transition energies and the splittings. However, the agreement between theory and experiment for symmetric stretch, mode 1, is singularly not very good. In every instance, however, the present results are much closer to experiment than those using the OSS3(p) potential.[38] For example, using that surface the calculated ground-state splittings for H_3O^+ and D_3O^+ are 15 and 3.8 cm^{-1}, respectively, compared to 41 and 10 cm^{-1} for the PES-2 potential. (The corresponding splittings for the higher barrier PES-1 are 35 and 8 cm^{-1}.) Fundamental transition energies were in disagreement with experiment by 100−300 cm^{-1}. In addition, the splitting of the fundamental ν_2 band experiences increases from 145 cm^{-1} for OSS3(p) to 338 cm^{-1} for the present PES-2 potential.

The trend of the experimental splittings in H_3O^+ is quite interesting and is well reproduced by the calculations. The experimental splittings increase in the order $\Delta\nu_4 > \Delta\nu_1 > \Delta\nu_3$, although the energies of these fundamentals are ordered in the reverse sequence. The calculations also show this trend, and a detailed analysis of this trend is possible using a vibrationally adiabatic model of the splittings. We plan to do that in the future; however, a simple indication that this analysis might work can be seen by considering the adiabatic inversion barrier height for a given mode. According to a harmonic vibrationally adiabatic theory, this barrier height is given by

$$E_{v_i}^{\ b} = V_0 + \hbar\left(v_i + \frac{1}{2}\right)\Delta\omega_i$$

where V_0 is the bare barrier height, v_i is the vibrational quantum number of mode i, and $\Delta\omega_i$ is the difference between the corresponding normal mode harmonic frequency at the saddle point and that at the minimum. From Table 3 we see that $\Delta\omega_4 = -60.0$, $\Delta\omega_1 = 82$, and $\Delta\omega_3 = 124$ cm^{-1}. Thus, the adiabatic barrier for mode 4 *decreases* with excitation in that mode but *increases* with excitation in modes 1 and 3. As a result, the expectation is the corresponding splittings would increase for mode 4 and decrease for modes 1 and 3 with excitation relative to the splitting with no excitation, i.e., the ground-state splitting. This is indeed seen in both experiment and in our vibrational calculations for H_3O^+. The same effect is also seen in the calculations for D_3O^+ and also for the one measured splitting for excited mode 3 for H_3O^+.

H_2DO^+ and HD_2O^+. MULTIMODE and RVIB4 calculations of the vibrational energies and of the splittings of the isotopomers H_2DO^+ and HD_2O^+ were done using PES-2, and the results are given in Table 5, along with the harmonic frequencies at the minimum. Note that MULTIMODE entries for ν_6 for H_2DO^+ are absent. The reason for this is that the MULTIMODE results are highly suspect for this excitation for the following reason. We noticed that the two ν_6 states were highly mixed in the MULTIMODE calculation, and that the mixing involved states with excitation in three modes other than mode 6. This high level of mode coupling is not accurately described by the four-mode representation of the potential used in MULTIMODE, and for this reason we do not include the results in the table. We did not find such mixing in MULTIMODE calculations for any other states in the table (nor in Table 4). With the exception of this state the agreement between MULTIMODE and RVIB4 energies is quite good.

No experimental data have been reported for these isotopomers, and so the results in Table 5 have to be regarded as "predictions". However, based on the comparisons between theory and experiment for H_3O^+ and D_3O^+, these predictions are not expected to be of "spectroscopic" accuracy, i.e., correct to with a few wavenumbers. We noticed that the calculated splittings for the ground state for both H_3O^+ and D_3O^+ are both roughly 70% of the experimental ones. If we assume that the same percentage error applies to H_2DO^+ and HD_2O^+, then we predict that the ground-state splittings for these molecules are 42 and 27 cm^{-1}, respectively. Interestingly, these adjusted splittings agree well with those reported from a calculation[34]

TABLE 5: Calculated H_2DO^+ and HD_2O^+ Vibrational Energies and Splittings (cm^{-1}) from MULTIMODE and RVIB4[a]

	H_2DO^+					HD_2O^+				
state	H.O.	sym	MM	RVIB4	splitting	H.O.	sym	MM	RVIB4	splitting
0(+)		A_1	6786	6791			A_1	6127	6134	
					29					27
0(−)		B_1	30	29			B_1	19	19	
ν_1(+)		A_1	541	539			A_1	502	502	
	614				282	562				222
ν_1(−)		B_1	824	821			B_1	724	724	
ν_2(+)		B_2	1369	1375			A_1	1229	1229	
	1360				37	1197				14
ν_2(−)		A_2	1408	1412			B_1	1244	1243	
ν_3(+)		A_1	1602	1607			B_2	1476	1475	
	1627				29	1495				22
ν_3(−)		B_1	1633	1636			A_2	1498	1497	
ν_4(+)		A_1	2555	2554			A_1	2504	2504	
	2737				23	2661				15
ν_4(−)		B_1	2580	2577			B_1	2520	2519	
ν_5(+)		A_1	3437	3438			B_2	2624	2620	
	3723				22	2819				8
ν_5(−)		B_1	3461	3460			A_2	2628	2628	
ν_6(+)		B_2		3516			A_1	3471	3475	
	3819				17	3774				11
ν_6(−)		A_2		3533			B_1	3482	3486	

[a] Zero-point energies are relative to the minimum, and all the other states are relative to it. Harmonic frequencies (H.O.) at the minimum are also given. Mode numbering is given in terms of increasing harmonic frequency.

based on the reduced dimensionality rigid-inverter model, in which the potential was adjusted to give the correct ground-state splittings for H_3O^+ and D_3O^+.

V. Summary and Conclusions

We reported new, extensive ab initio CCSD(T) calculations of the energies of H_3O^+ using large polarized basis sets. Potential energy surfaces were obtained by least-squares fits to these energies. The potential based on a combination of aug-cc-PVTZ and aug-cc-PVQZ electronic bases was used in full dimensional vibrational calculation splittings of the ground state, fundamentals, and first overtone of the umbrella mode for H_3O^+ and D_3O^+ using two codes, RIVIB4 and MULTIMODE. The vibrational energies and splittings from MULTIMODE were in very good agreement with the exact results from RVIB4. Agreement with all the available experimental data was generally good, with the splittings calculated somewhat smaller than those measured. This might be due to the inversion barrier height of the fitted potential (693 cm^{-1}) being slightly high. Vibrational energies using MULTIMODE and RVIB4 were obtained for the isotopomers H_2DO^+ and HD_2O^+, for which no experimental data exist.

The calculation of vibrational energies of a molecule with large splittings, of which H_3O^+ is an example, is quite challenging because the splittings greatly affect the energies of the fundamentals. Thus, to accurately describe even the low-lying vibrational states, it is essential to consider the properties of the potential surface in a wide region between the potential minima and inversion saddle point. There is a corresponding challenge for methods to obtain the vibrational energies, since these methods must be capable of describing coupled motion over the region of the minima and the saddle point. We have shown that the modification of MULTIMODE to do this, by using normal modes of the saddle point, is capable of describing this motion for H_3O^+ accurately.

Acknowledgment. Financial support from Office of Naval Research (ONR-N00014-01-1-0235) is gratefully acknowledged. X.H. thanks Celine Leonard for very helpful discussions about the fitting of ab initio energies.

References and Notes

(1) Smith, J. A. S. *Q. Rev. Chem. Soc. London* **1953**, *7*, 279.
(2) Eigen, M. *Angew. Chem., Int. Ed. Engl.* **1964**, *3*, 1.
(3) Herbst, E.; Klemperer, W. *Astrophys. J.* **1973**, *185*, 505.
(4) Jong, T. de.; Dalgarno, A.; Boland, W. *Astron. Asrophys.* **1980**, *91*, 68.
(5) Koeppl, G. W.; Sagatys, D. S.; Krishnamurthy, G. S.; Miller, S. I. *J. Am. Chem. Soc.* **1967**, *89* (14), 3396.
(6) Schwarz, H. A. *J. Chem. Phys.* **1977**, *67*, 5525.
(7) Begemann, M. H.; Gudeman, C. S.; Pfaff, J.; Saykally, R. J. *Phys. Rev. Lett.* **1983**, *51* (7), 554.
(8) Gruebele, M.; Polak, M.; Saykally, R. J. *J. Chem. Phys.* **1987**, *87*, 3347.
(9) Tang, J.; Oka, T. *J. Mol. Spectrosc.* **1999**, *196*, 120.
(10) Haese, N. N.; Oka, T. *J. Chem. Phys.* **1984**, *80* (1), 572.
(11) Liu, D.; Oka, T. *Phys. Rev. Lett.* **1985**, *54* (16), 1787.
(12) Davies, P. B.; Hamilton, P. A.; Johnson, S. A. *J. Opt. Soc. Am. B: Opt. Phys.* **1985**, *2* (5), 794.
(13) Davies, P. B.; Johnson, S. A.; Hamilton, P. A.; Sears, T. J. *Chem. Phys.* **1986**, *108*, 335.
(14) Liu, D.; Haese, N. N.; Oka, T. *J. Chem. Phys.* **1985**, *82* (12), 5368.
(15) Verhoeve, P.; Versluis, M.; Ter Meulen, J. J.; Meerts, W. L.; Dymanus, A. *Chem. Phys. Lett.* **1989**, *161* (3), 195.
(16) (a) Sears, T. J.; Bunker, P. R.; Davies, P. B.; Johnson, S. A.; Spirko, V. *J. Chem. Phys.* **1985**, *83*, 2676. (b) Araki, M.; Ozeki, H.; Saito, S. *J. Chem. Phys.* **1998**, *109*, 5707.
(17) Petek, H.; Nesbitt, D. J.; Owrutsky, J. C.; Gudeman, C. S.; Yang, X.; Harris, D. O.; Moore, C. B.; Saykally, R. J. *J. Chem. Phys.* **1990**, *92*, 3257.
(18) Ferguson, W. I.; Handy, N. C. *Chem. Phys. Lett.* **1980**, *71*, 95.
(19) Heinzinger, K.; Weston, R. E. *J. Phys. Chem.* **1964**, *68*, 744.
(20) Bishop, D. M. *J. Chem. Phys.* **1965**, *43*, 4453.
(21) Koeppl, G. W.; Sagatys, D. S.; Krishnamurthy, G. S.; Miller, S. I. *J. Am. Chem. Soc.* **1967**, *89*, 3396.
(22) Kebarle, P.; Searles, S. K.; Zolla, A.; Scarborough, J.; Arshadi, M. *J. Am. Chem. Soc.* **1967**, *89*, 6393.
(23) Paz, M. de; Leventhal, J. J.; Friedman, L. *J. Chem. Phys.* **1969**, *51*, 3748.
(24) Almlof, J.; Wahlgren, U. *Theor. Chim. Acta* **1973**, *28*, 161.
(25) Kollman, P. A.; Bender, C. F. *Chem. Phys. Lett.* **1973**, *21*, 271.
(26) Lischka, H.; Dyczmons, V. *Chem. Phys. Lett.* **1973**, *23*, 167.
(27) Basile, L. J.; LaBonville, P.; Ferraro, J. R.; Williams, J. M. *J. Chem. Phys.* **1974**, *60*, 1981.
(28) Stevenson, P. E.; Burkey, D. L. *J. Am. Chem. Soc.* **1974**, *96*, 3061.
(29) Ahlrichs, R.; Driessler, F.; Lischka, H.; Staemmler, V.; Kutzelnigg, W. *J. Chem. Phys.* **1975**, *62*, 1235.
(30) (a) Spirko, V.; Bunker, P. R. *J. Mol. Spectrosc.* **1982**, *95*, 226. (b) Spirko, V. *J. Mol. Spectrosc.* **1983**, *101*, 30.
(31) (a) Bunker, P. R.; Amano, T.; Spirko, V. *J. Mol. Spectrosc.* **1984**, *107*, 208. (b) Bunker, P. R.; Kraemer, W. P.; Spirko, V. *J. Mol. Spectrosc.* **1983**, *101*, 180.

(32) Danielis, V.; Spirko, V. *J. Mol. Spectrosc.* **1986**, *117*, 175.
(33) Spirko, V.; Kreamer, W. P. *J. Mol. Spectrosc.* **1989**, *134*, 72.
(34) Spirko, V.; Kreamer, W. P. *J. Mol. Spectrosc.* **1989**, *133*, 331.
(35) Gomez, M. A.; Pratt, L. R. *J. Chem. Phys.* **1998**, *109*, 8783.
(36) Stillinger, F. H.; Stillinger, D. K.; Hodgdon, J. A. Quoted in ref 35 as a private communication.
(37) Ojamae, L.; Shavitt, I.; Singer, S. J. *J. Chem. Phys.* **1998**, *109*, 5547.
(38) Bowman, J. M.; Huang, X.; Carter, S. *Spectrochim. Acta A* **2002**, *58*, 839.
(39) Ojamae, L.; Shavitt, I.; Singer, S. J. *Int. J. Quantum Chem.: Quantum Chem. Symp.* **1995**, *29*, 657.
(40) Martin, R. L.; Hay, P. J.; Pratt, L. R. *J. Phys. Chem.* **1998**, *102*, 3565, as cited in ref 39.
(41) Handy, N. C.; Carter S.; Colwell, S. M. *Mol. Phys.* **1999**, *96*, 477.
(42) Léonard, C.; Handy, N. C.; Carter, S.; Bowman, J. M. *Spectrochim. Acta A* **2002**, *58*, 825.
(43) Carter, S.; Culik, S. J.; Bowman, J. M. *J. Chem. Phys.* **1997**, *107*, 10458.
(44) Carter, S.; Bowman, J. M. *J. Chem. Phys.* **1998**, *108*, 4397.
(45) Carter, S.; Bowman, J. M.; Handy, N. C. *Theor. Chem. Acc.* **1998**, *100*, 191.
(46) Online documents and a more extensive list of references can be found at http://www.emory.edu/CHEMISTRY/faculty/bowman/multimode.
(47) (a) MOLPRO 2000.1 is a suite of ab initio programs written by H.-J. Werner and P. J. Knowles with contributions from R. D. Amos, A. Bernhardsson, A. Berning, P. Celani, D. L. Cooper, M. J. O. Deegan, A. J. Dobbyn, F. Eckert, C. Hampel, G. Hetzer, T. Korona, R. Lindh, A. W. Lloyd, S. J. McNicholas, F. R. Manby, W. Meyer, M. E. Mura, A. Nicklass, P. Palmieri, R. Pitzer, G. Rauhut, M. Schütz, H. Stoll, A. J. Stone, R. Tarroni, and T. Thorsteinsson. (b) Geometry optimization: Eckert, F.; Pulay, P.; Werner, H.-J. *J. Comput. Chem.* **1997**, *18*, 1473. (c) Coupled-Cluster treatments: Hampel, C.; Peterson, K.; Werner, H.-J. *Chem. Phys. Lett.* **1992**, *190*, 1 and references therein. The program to compute the perturbative triples corrections has been developed by: M. J. O. Deegan and P. J. Knowles in 1992. (d) Hampel, C.; Werner, H.-J. *J. Chem. Phys.* **1996**, *104*, 6286. Hetzer, G.; Pulay, P.; Werner, H.-J. *Chem. Phys. Lett.* **1998**, *290*, 143. Schütz, M.; Hetzer, G.; Werner, H.-J. *J. Chem. Phys.* **1999**, *111*, 5691.
(48) Kendall, R. A.; Dunning, T. J., Jr.; Harrison, R. J. *J. Chem. Phys.* **1992**, *96*, 6796.
(49) (a) Watson, J. K. G. *Mol. Phys.* **1968**, *15*, 479. (b)Watson, J. K. G. *Mol. Phys.* **1970**, *19*, 465.